



An Intelligent Adaptive Overcurrent Protection System for an Automated Microgrid in Islanded and Grid-Connected Operation Modes

Mahmood Sadoughi, Mehrdad Hojjat*, Mohamad Hosseini Abardeh

Department of Electrical and Electronic Engineering, Shahrood Branch, Islamic Azad University, Shahrood, Iran.

(Communicated by Madjid Eshaghi Gordji)

Abstract

As the penetration of distributed generation sources increases at the distribution level, the necessity of designing microgrids is highlighted. Microgrids can operate in either islanded (separated from the utility grid) or grid-connected mode. Apart from the technical and economic benefits of microgrids, they may cause some protection issues in distribution systems. The most important of these issues is the difference between the short circuit levels in islanded and grid-connected operation modes. In this paper, an intelligent overcurrent relay that can adapt to the microgrid operation mode is proposed; that is, the relay detects the microgrid operation mode by means of an adaptive algorithm. The proposed adaptive method optimizes the accuracy and speed of the algorithm for detecting the microgrid operation mode. Then, the optimal settings that have been already stored in the relay are activated according to the microgrid operation mode. All internal processes of the relay use the voltage and current sampled at the relay location. As a result, the relay can be used in all networks without communication infrastructures. Finally, the proposed method is implemented in a sample microgrid. The superiority of the intelligent relay performance over conventional overcurrent relays is shown by numerical results.

Keywords: Overcurrent Relay, Microgrid, Islanded operation, Adaptive Algorithm, Coordination, Convolutional Neural Network.

2010 MSC: 68T05,62M45

*Mehrdad Hojjat

Email address: m.sadoughi@iau-shahrood.ac.ir, mehrdad.hojat@iau-shahrood.ac.ir, mohamad.hosseini@mail.um.ac.ir (Mahmood Sadoughi, Mehrdad Hojjat*, Mohamad Hosseini Abardeh)

Received: December 2019 *Revised:* February 2020

1. Introduction

A microgrid is a small power system that includes some distributed generation (DG) sources and loads at the distribution level. The microgrid is connected to the grid at the point of common coupling (PCC). As a feature, microgrids can supply their local loads in the islanded mode of operation [1]. Despite many advantages, the use of microgrids causes some protection challenges that do not occur in conventional distribution systems [2].

Protection planning for microgrids is an important challenge. A protection scheme must meet the essential requirements of the network, such as operation coordination, sensitivity and reliability for both grid-connected and islanded modes of operation. Accordingly, protection schemes are divided into two general categories, i.e., adaptive and robust schemes [3]. In robust schemes, identical protection settings are provided for both islanded and grid-connected modes of operation. However, in adaptive schemes, individual protection settings are implemented for each operation mode of the microgrid [4].

An adaptive method is proposed in [5] to maintain coordination of the operation of fuses and inverse time relays. To maintain relays coordination, adaptive approaches [6, 7] require data exchange through communication links. The need for communication links is less in the approach proposed in [6]. In [8], a neural network-based algorithm is proposed that uses the measurements across the network to coordinate the overcurrent relays operation.

In [9], each directional overcurrent relay has two operation characteristics for forward and reverse faults. Using a communication system, each relay can enable different settings for proper operation in each operation mode of the microgrid. In [10], protection relays are connected to DG sources by conventional microgrid communication mediums (MCMs). References [11, 12] present a method for controlling the fault current supplied by a voltage source converter (VSC). In these cases, the predetermined coordination and sensitivity are maintained for conventional overcurrent protection devices in the network. In an adaptive method presented in [13], the microgrid operation mode is detected by injecting perturbation through thyristors at the relay location. Then, the relay settings are updated based on the islanding detection algorithm in active methods.

In most recent studies, the adaptive schemes have been employed to improve the overcurrent relays operation using communication systems. However, communication and automation infrastructures in current Iran's distribution systems cannot employ adaptive plans based on communication medium. Moreover, the implementation of decentralized plans and building the infrastructures require considerable investment.

This paper presents an intelligent relay with an adaptive algorithm. This relay uses only the voltage and current at the relay location and does not need communication systems. In the proposed adaptive algorithm, the microgrid operation mode has to be detected first, and the appropriate relay settings have to be activated accordingly. To detect the microgrid operation mode, an algorithm based on a convolutional neural network (CNN) with the optimal structure is used.

The algorithm for detecting the microgrid connection status (operation mode) consists of two parts, i.e., a classifier and an optimizer. The classifier uses the CNN, and as its most important advantage, it is free from feature extraction and feature selection. Feature extraction is performed automatically in the CNN. In this method, the voltage signal is used as the input to the CNN. Furthermore, there are many parameters in the CNN such as the number of convolutional layers, the number of filters and filter size that must be correctly determined in order for the proper operation of the CNN. Accordingly, the optimizer of the bees optimization algorithm determines these parameters.

2. Overcurrent relays coordination problem

Inverse time overcurrent relays are the most commonly used type of overcurrent relays. Their operating time (OT) is a function of the current passing through the relay; that is, as the fault current increases, the relay OT decreases. The operating characteristic of these relays is expressed in (2.1) according to the IEC standard. Coefficients A and B determine the type of inverse time curve.

$$T_{op} = \frac{A \times TMS}{\left(\frac{I_F}{I_{set}}\right)^B - 1} \quad (2.1)$$

Where I_{set} denotes the current setting and TMS stands for the time multiplier setting of the relay; these are the unknowns of the coordination problem. The coordination problem is usually intended to minimize the OT of the primary protection. The coordination problem has some constraints, of which the most important is the minimum coordination time interval (CTI) between the OTs of the backup and primary relays.

Consequently, in the case of a change in the operation mode of a microgrid, and therefore, the fault current through the lines and relays, the OTs of the overcurrent relays and the relay pairs coordination are greatly affected.

2.1. Protection issues caused by microgrids

Short circuit levels are different for each microgrid operation mode (islanded and grid-connected modes) [14]. In grid-connected operation mode, the fault current is very high for a fault occurrence within the utility grid due to the high short circuit level of the grid and the presence of DG sources. However, for a fault occurrence in islanded operation mode of the microgrid, the fault current is only supplied by the sources within the microgrid, so the fault current magnitude is greatly reduced [15]. As a result, relays OT, sensitivity and protection coordination are severely affected [16].

2.2. Proposed approach for maintaining relay pairs coordination

In this paper, a novel intelligent adaptive method is proposed to modify the settings of a relay for each microgrid operation mode. The relay has two main parts. The first part detects fault and operation mode in a very similar way to the conventional inverse time overcurrent relays. The second part, which includes the adaptive unit of the relay, is optimally designed based on the proposed algorithm to maximize the accuracy of the adaptive algorithm while minimizing the relay operating speed. The overall schematic of the proposed method is shown in Fig. 1. The processes needed to implement the proposed method are divided into two categories of online and offline calculations. Offline calculations determine the design parameters of the intelligent relay.

Two sets of settings are calculated and stored offline for each relay; the first set for islanded and the second one for grid-connected operation mode. Moreover, the optimal structure of CNN (the values of its setting parameters) must be determined by the bees algorithm.

Other processes have to be executed in the relay algorithm (inside the relay) continuously and online. The relay algorithm is divided into two parallel sections. One section detects and stores microgrid operation mode at given time intervals (T_s) using CNN. Since the microgrid operation mode is detected separately, it does not affect the fault detection time and the OT of the relay.

The other (parallel) section measures voltage and current momentarily at the relay location. Then, according to the microgrid connection status (the last CNN output), the appropriate relay settings are activated. Next, it should be examined if a fault has occurred in the network. In the case of a fault, the relay OT is calculated and an appropriate command is sent to the corresponding

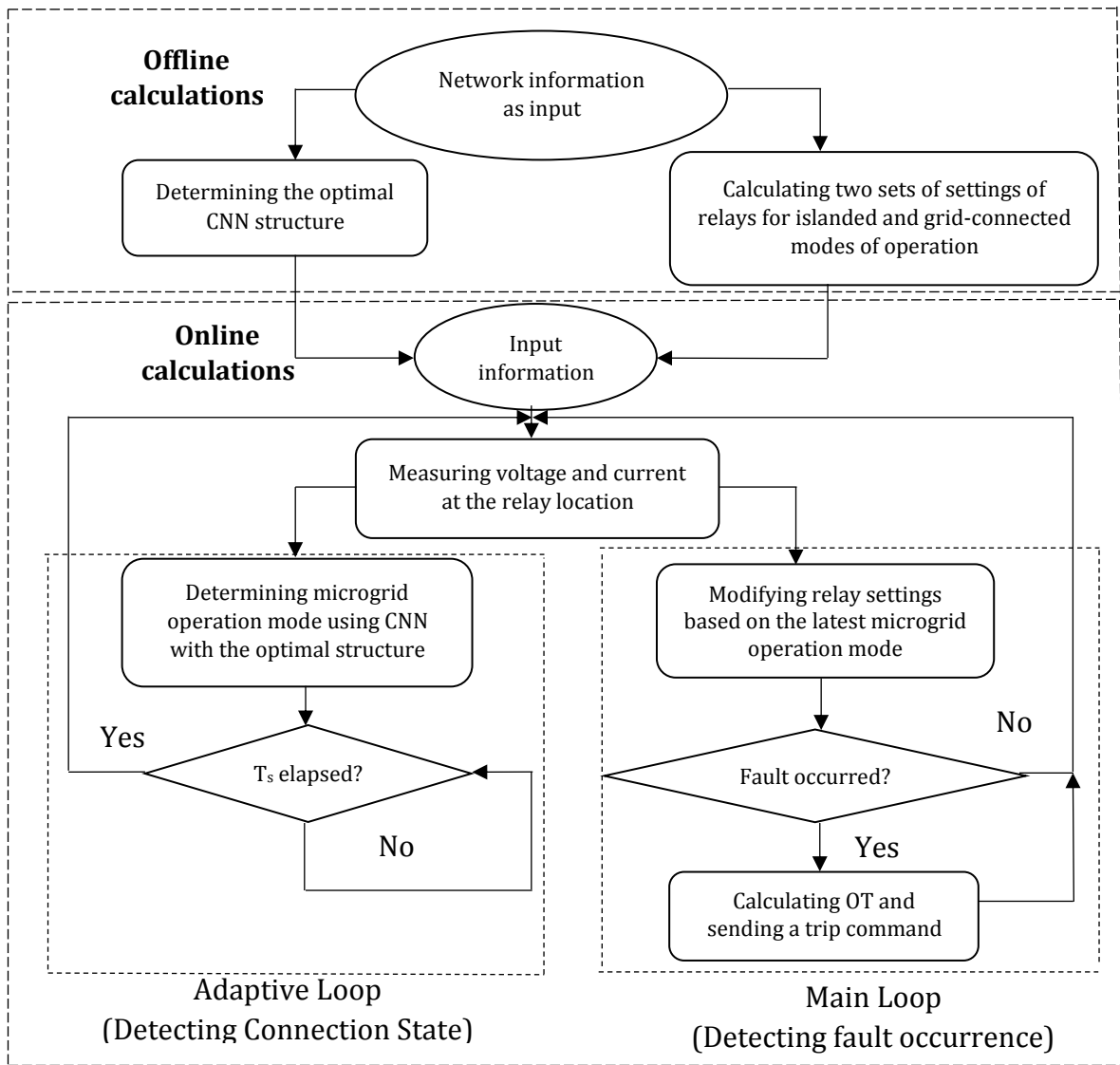


Figure 1: Flowchart of the proposed algorithm

circuit breaker; otherwise, the relay algorithm is repeated. In the following, the required calculations for the optimal design of the proposed intelligent relay are explained in detail.

3. Optimal design of proposed intelligent relay

The intelligent relay is built using the results from the offline part. The overall algorithm for determining the optimal CNN structure that detects the microgrid operation mode is shown in Fig. 2. The bees algorithm is also used to find the optimal parameters of the convolutional neural network.

Some parameters in the structure of CNN highly affect the performance and accuracy of the neural network. These parameters are generally related to:

1. Network architecture: number of hidden layers (NHL), learning rate (α) and type of pooling layer (TPL)
2. Convolutional layer: number of filters (K), filter size (F), step size (S) and zero padding (P)
3. Polling layer: filter size (F) and step size (S)

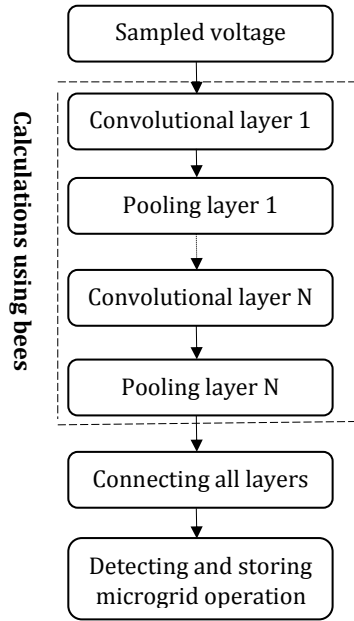


Figure 2: Algorithm for designing CNN to determine microgrid operation mode

The number of these parameters increases with the number of layers. Each bee has to represent the number of hidden layers and the other parameters of the network. In this paper, the maximum number of hidden layers is six. There are seven parameters in each hidden layer, so, considering the parameters of the number of layers and the learning rate, each bee has 43 segments. The optimal values of these variables must be found so that the CNN has the highest accuracy. Figure 3 shows a sample bee.

NHL	a	K _c	F _c	S _c	P _c	F _p	S _p	...	F _p	S _p	K _c	F _c	S _c	P _c	F _p	S _p
-----	---	----------------	----------------	----------------	----------------	----------------	----------------	-----	----------------	----------------	----------------	----------------	----------------	----------------	----------------	----------------

Figure 3: Structure of bees for optimally designing CNN

The objective function (the fitness function of each bee) is considered as the accuracy rate of CNN detections according to (3.1). This index (PF) is defined as the ratio of false detections (FD) to total detections (FD + TD). Obviously, the bees algorithm evolves to minimize PF and to maximize the true detections.

$$PF = \frac{FD}{TD + FD} \tag{3.1}$$

4. Simulation results

For numerical evaluation and verification, the proposed method is implemented in a sample microgrid with 12 overcurrent relays.

The microgrid has four DG sources (synchronous-based, DFIG and inverter-based) that can be connected to the upstream network. Full network specifications are available in [17]. Table 1 lists all operating conditions and events that are used to train and evaluate the CNN. In sum, 9280 events are simulated of which 300 correspond to islanded and 300 to the grid-connected operation mode. Seventy percent of all data are dedicated for training the CNN and the remaining 30% for evaluating its performance

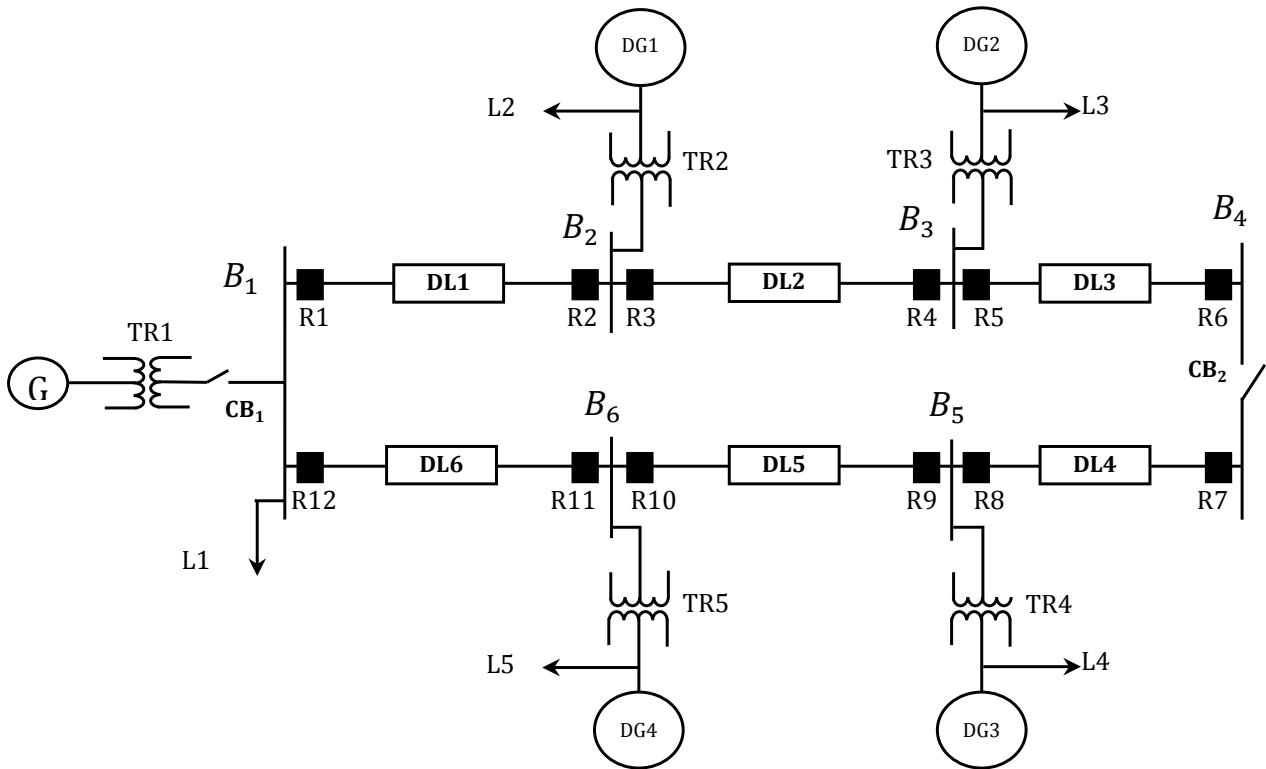


Figure 4: Microgrid under study [17].

Table 1: Different events and operating conditions of microgrid

Event type	Number of states	Operating conditions	Number of states
Connection/disconnection of DG sources (DG1, DG2, DG3 and DG4)	10	Change in network configuration (ring/radial)	2
Connection/disconnection of loads (L1, L2, L3, L4, L5 and L6)	22	Generation-consumption balance / $\pm 10\%$ and $\pm 20\%$ imbalance	5
Microgrid operation mode	2	Change in power factor of loads	3
Occurrence of one-, two- and three-phase faults with different impedances	6	Microgrid operation mode	2
		Disconnection of one DG	5

4.1. CNN performance with non-optimal structure

In this subsection, the performance of the CNN is compared with some non-optimal structures as shown in Table 2. In this table, different values of filter size, number of filters, number of convolutional layers, type of pooling function, learning rate, etc. are determined and the accuracy of the CNN is calculated for each case. Moreover, the SD index, which has high values, represents the standard deviation of the CNN performance over 50 runs. The highest accuracy (97.18%) is obtained for three convolutional layers.

The results indicate that the performance of CNN depends on the number of filters, their size, etc. although there is no definite relationship between the parameters and the network accuracy. For

Table 2: Performance evaluation of some non-optimal structures of CNN.

NHL	Layer	a	TPL	K _c	F _c	S _c	P _c	F _p	S _p	SD	Accuracy
1	1	0.01	Max	10	4	1	1	5	1	±1.19	88.75
1	1	0.005		10	4	1	1	5	1	±1.14	91.25
2	1			10	4	1	1	5	1	±0.81	96.31
	2			12	3	1	1	3	1		
2	1		average	10	4	1	1	5	1	±0.87	96.18
	2			14	3	1	2	2	1		
3	1		Max	10	4	1	1	5	1	±0.49	97.18
	2			12	3	1	1	3	1		
	3			18	3	1	1	3	1		
3	1		L2-norm	10	4	1	1	5	1	±0.53	96.87
	2			14	3	2	2	2	1		
	3			24	3	1	1	3	1		

example, it cannot be concluded that a reduction in the number of filters increases or decreases the accuracy of the network, so the value of this parameter has to be determined so that the best result is obtained.

Table 3 presents the overlapping matrix of the CNN detections in a structure with an accuracy of 97.18%. The main diagonal elements indicate the number of correct (true) detections, and other elements indicate the number of incorrect (false) detections. For example, 651 in Row 1 represents the number of islanded modes that have been correctly detected and 17 indicates the number of islanded modes that have been incorrectly detected as normal operation.

Table 3: Overlapping matrix of CNN detections with an accuracy of 97.18%.

	Islanded	Reconnection	Other events
Islanded	65	3	11
Reconnection	2	73	4
Other events	45	13	2546

4.2. CNN performance with optimal structure

The analyses in the previous subsection prove the necessity of determining the optimal values of the CNN parameters. Accordingly, a bees algorithm with the structure shown in Table 4 is used to optimize the performance and design of CNN layers.

Table 4: Values of bees algorithm parameters.

Number of bees (n)	30
Number of elite bees (m)	8
Number of elite bees in Group 1 (e)	4
Number of foragers for the elite bee in Group 1 (nep)	3
Number of foragers for the elite bee in Group 2 (nsp)	3
Maximum number of iterations	100

According to the optimized results of the bees algorithm, the best CNN structure should have five hidden layers with a learning rate of 0.0037. A maximum pooling function is chosen, which has an accuracy of 99.8%. Other specifications are listed in Table 5.

Table 5: Proposed optimal structure by bees algorithm.

Pooling layer			Convolutional layer				Number of filters	Layer No.
S _p	F _p	Structure	P _c	S _c	F _c	Structure		
		---				60*1	---	0
1	8	52*6	1	1	4	59*6	6	1
1	3	49*14	2	1	6	51*14	14	2
1	3	23*10	2	2	3	25*10	10	3
2	4	10*16	1	1	6	20*16	16	4

The overlapping matrix of CNN detections with the optimal structure is given in Table 6. As can be seen, the number of false detections has decreased significantly. All reconnection events are correctly detected. However, only two islanding events out of the 79 that have been randomly selected to evaluate the CNN performance have been incorrectly detected as other events.

Table 6: Overlapping matrix of CNN detections with the optimal structure.

	Islanded	Reconnection	Other events
Islanded	78	0	2
Reconnection	0	79	0
Other events	5	0	2605

4.3. Comparison with other classifiers

In Table 7, the performance of the CNN in determining the microgrid connection status is compared with the performances of other classifiers including perceptron neural networks with error back propagation (BP) learning, Levenberg Marquardt (LM), resilient propagation (RP), radial basis function neural network (RBFNN), probabilistic neural network (PNN) and artificial neural network fuzzy inference system (ANFIS). In this comparison, the voltage vector is used as the input of all classifiers. It is observed that the proposed method has the minimum standard deviation and the highest accuracy compared to other methods.

4.4. Determining optimal relay settings

Fault currents through the relay are given in Table 8 for both microgrid operation modes. Indices A and B indicate fault occurrences immediately next to the primary relay and at the end of the primary relay line. Moreover, indices Is and Gr indicate the islanded and grid-connected operation modes; as can be seen, the short circuit levels are very different in these modes.

The bees algorithm is used again to determine the optimal settings of the relays. The exceptions are as follows. First, the objective function must be defined as the sum of the overcurrent relays OTs. Second, coordination constraints must be added to the problem. Third, the structure of the bees must be changed according to Fig. 5. Each bee has 2N segments, where N is the total number of overcurrent relays.

Table 7: Comparison of the performances of CNN and other classifiers.

Classifier	Parameters	Number of inputs	Accuracy (percent)	Standard Deviation (percent)
PNN	Spread=0.5	600	93.26	± 2.16
MLP (BP)	No. hidden layers=2 No. neurons in the 1st hidden layer=15 No. neurons in the 2nd hidden layer=23 Learning rate= 0.001 Activation Function= Sigmoid	600	91.43	± 3.70
MLP (RP)	No. hidden layers=3 No. neurons in the 1st hidden layer=18 No. neurons in the 2nd hidden layer=20 No. neurons in the 3rd hidden layer=13 Learning rate= 0.001 Activation Function= Sigmoid	600	95.24	± 1.43
MLP (LM)	No. hidden layers=2 No. neurons in the 1st hidden layer=9 No. neurons in the 2nd hidden layer=16 Learning rate= 0.001 Activation Function= Sigmoid	600	96.17	± 1.28
RBFNN	No. RBFs= 75 Spread= 1	600	96.62	± 1.21
ANFIS	Membership function= Gaussian System= Sugeno Radii= 0.2	600	96.81	± 0.78
CNN	Table 6	600	99.80	± 0.0

Table 8: Currents through relays in both microgrid operation modes.

Backup relay current (in per unit)					Primary relay current (in per unit)					Relay pair No.
Fault at B		Fault at A		Relay No.	Fault at B		Fault at A		Relay No.	
Is	Gr	Is	Gr		Is	Gr	Is	Gr		
1.87	0.65	2.78	2.71	11	2.05	6.51	3.14	22.22	1	1
1.27	1.29	2.38	2.89	4	2.8	2.82	4.49	4.99	2	2
1.16	3.28	2.03	6.4	1	2.41	4.32	3.9	8.38	3	3
0.81	1.46	1.75	2.49	6	2.4	2.92	3.84	4.56	4	4
1.3	2.47	2.39	4.27	3	2.73	3.69	4.41	6.28	5	5
1.77	2.51	2.7	3.66	8	1.77	2.51	2.7	3.66	6	6
1.77	2.51	2.7	3.66	5	1.77	2.51	2.7	3.66	7	7
1.3	2.47	2.39	4.27	10	2.73	3.69	4.41	6.28	8	8
0.81	1.46	1.75	2.49	7	2.4	2.92	3.84	4.56	9	9
1.16	3.28	2.03	6.4	12	2.41	4.32	3.9	8.38	10	10
1.27	1.29	2.38	2.89	9	2.8	2.82	4.49	4.99	11	11
1.87	0.65	2.78	2.71	2	2.05	6.51	3.14	22.22	12	12

Two sets of optimal settings are given in Table 9 for all relays in islanded and grid-connected operation modes. When the microgrid operation mode changes, the conventional relays may face

$I_{Set_1}^1$	TSM_1^1	$I_{Set_2}^1$	TSM_2^1	...	$I_{Set_N}^1$	TSM_N^1
---------------	-----------	---------------	-----------	-----	---------------	-----------

Figure 5: Structure of bees in the overcurrent relays coordination problem.

miscoordination due to their inappropriate settings. Relay pairs coordination is investigated in Table 10 for the two microgrid operation modes. Indices MR and BR represent, respectively, the primary and backup relays. The difference between the OTs of the primary and backup relays is shown with the DT index.

As can be seen, either the relays do not operate at all (reduction in short circuit level) or at least the allowable difference of relay pair OTs is violated, so miscoordination occurs.

Table 9: Optimal overcurrent relays settings.

No of MR	No of BR	Grid-connected mode						Islanded mode					
		TSM	I _{Set}	t _{MR} (s)	TSM	I _{Set}	t _{BR} (s)	TSM	I _{Set}	t _{MR} (s)	TSM	I _{Set}	t _{BR} (s)
1	11	0.11	2	0.3121	0.0718	1.2	0.6120	0.0465	1.2	0.3349	0.0358	1.875	0.6334
2	4	0.0718	1.2	0.3473	0.0754	1.288	0.6477	0.0358	1.8745	0.2848	0.0527	1.271	0.5840
3	1	0.0735	2	0.354	0.11	2	0.6543	0.0498	1.303	0.3143	0.0465	1.2	0.6159
4	6	0.0754	1.288	0.4123	0.0544	1.464	0.7128	0.0527	1.2704	0.3299	0.0339	1.2	0.6266
5	3	0.0618	2	0.3734	0.0735	2	0.6732	0.036	1.7663	0.2726	0.0498	1.303	0.5712
6	8	0.0544	1.464	0.4123	0.0618	2	0.7115	0.0339	1.2	0.2895	0.036	1.766	0.5910
7	5	0.0544	1.464	0.4123	0.0618	2	0.7115	0.0339	1.2	0.2895	0.036	1.766	0.5913
8	10	0.0618	2	0.3734	0.0735	2	0.6732	0.036	1.7659	0.2727	0.0498	1.303	0.5710
9	7	0.0754	1.3	0.4123	0.0544	1.464	0.7127	0.0527	1.2704	0.3299	0.0339	1.2	0.6266
10	12	0.0735	2	0.354	0.11	2	0.6543	0.0498	1.3028	0.3144	0.0465	1.2	0.6159
11	9	0.0718	1.2	0.3473	0.0754	1.3	0.6554	0.0358	1.8745	0.2847	0.0527	1.270	0.5840
12	2	0.11	2	0.3121	0.0718	1.2	0.6120	0.0465	1.2	0.335	0.0358	1.875	0.6334
Total (seconds)		---	---	4.4228	---	---	8.0307	---	---	3.6522	---	---	7.2441

To compare the performances of conventional overcurrent relays and the proposed intelligent relay, it is assumed that the microgrid is islanded and the corresponding settings are stored in the relays. However, due to a change in the structure, the microgrid operation mode becomes grid-connected. In this case, an increase in the short circuit level decreases the OTs of all relays, and since the reduction in backup relays OTs is greater, all relay pairs are miscoordinated. This can also be observed in the results of Table 10. Since DT is negative for all relay pairs in the grid-connected operation mode for fault occurrence at location A, the coordination between all relay pairs fails.

If relay settings are adjusted for grid-connected operation mode, and an islanding event occurs followed by a fault at the end of the line, then all backup relays will not operate due to a severe fault current reduction. Consequently, the backup protection fails completely. However, under these conditions, the OTs of the primary relays increase considerably. Similarly, if the relay settings are initially adjusted for islanded operation, then a reconnection and fault occurrence lead to negative DT; that is, miscoordination occurs in the operation of most of the relay pairs.

However, if these relays employ the proposed algorithm, all of these issues will be resolved. For example, if the relay pair R3 and R1 are adjusted for islanded operation, the OTs of this pair are 0.18 and 0.19 seconds, respectively; these values are obtained for a fault occurrence at the beginning of the line (location A) when the microgrid is in grid-connected operation mode. As shown in Fig. 6, the time difference between OTs of this relay pair has decreased to 0.01 and the DT to minus 0.293. Consequently, the relay pair miscoordination is highly likely

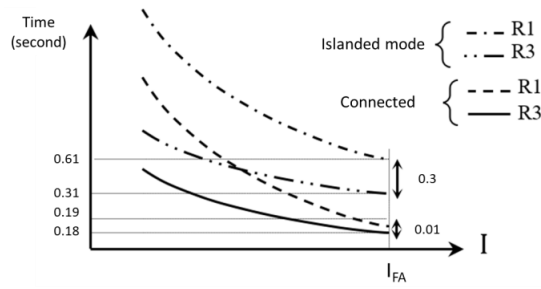


Figure 6: Comparison of OTs of relay pair R1 and R3.

Table 10: Miscoordination due to a change in microgrid operation mode.

Reconnection						Islanding						BR No.	MR No.
Fault at B			Fault at A			Fault at B			Fault at A				
DT	BR	MR	DT	BR	MR	DT	BR	MR	DT	BR	MR		
---	---	0.19	0.27	0.68	0.11	---	---	---	-1.405	0.59	1.7	11	1
26.10	27	0.16	-0.1	0.4	0.25	---	---	0.59	0.2	0.9	0.38	4	2
---	---	---	-0.293	0.19	0.18	---	---	2.73	47.04	48.11	0.77	1	3
---	---	---	-0.263	0.32	0.29	---	---	0.48	1.38	2.16	0.48	6	4
-0.097	0.54	0.43	-0.206	0.29	0.2	---	---	1.93	2.07	2.91	0.54	3	5
0.09	0.71	0.32	-0.167	0.34	0.21	---	---	2.02	0.51	1.43	0.62	8	6
0.09	0.71	0.32	-0.167	0.34	0.21	---	---	2.02	0.51	1.43	0.62	5	7
-0.097	0.54	0.34	-0.206	0.29	0.2	---	---	1.39	2.07	2.91	0.54	10	8
---	---	---	-0.263	0.32	0.29	---	---	0.84	1.38	2.16	0.48	7	9
---	---	---	-0.293	0.19	0.18	---	---	2.73	46.75	47.82	0.77	12	10
26.10	27	0.61	-0.1	0.4	0.25	---	---	0.59	0.2	0.9	0.38	9	11
---	---	0.19	0.27	0.68	0.11	---	---	---	-1.404	0.59	1.7	2	12

5. Conclusion

The need for revising the protection systems in the presence of microgrids is a major challenge. The OTs and coordination of overcurrent relays highly depend on the current passing through the relays. In this paper, an intelligent overcurrent relay was proposed for detecting microgrid operation mode using a convolutional neural network (CNN). Based on the microgrid operation mode, the relay activates the corresponding settings that maintain relays coordination. The CNN structure is optimized by the bees algorithm. Based on the numerical results, it was found that in the case of a change in the microgrid operation mode, the short circuit levels of faults change significantly, and relay pairs miscoordination and non-operation may occur. However, if the overcurrent relays include the proposed intelligent adaptive algorithm, they can detect the microgrid operation mode and update their settings only by measuring the information at the relay location.

References

[1] J. M. Guerrero et al., "DG: Toward a new energy paradigm," IEEE Industrial Electronics Magazine, vol. 1, no. 4, pp. 52-64, 2010.
 [2] A. Gholami, F. Aminifar, and M. Shahidehpour, "enhancing the resilience of the electricity grid through microgrid facilities," IEEE Electrification Magazine, vol. 4, no. 1, pp. 18-24, 2016.
 [3] M. A. Zamani, T. S. Sidhu, and A. Yazdani, "A protection strategy and microprocessor-based relay for low-voltage microgrids," Power delivery, IEEE transactions on, vol. 26, no. 3, pp. 1873-1883,

2011.

- [4] A. H. Etemadi and R. Iravani, "Overcurrent and overload protection of directly voltage-controlled DRs in a microgrid," *Industrial Electronics, IEEE Transactions on*, vol. 60, no. 12, pp. 5629-5638, 2013.
- [5] E. C. Piesciorovsky and N. N. Schulz, "Fuse relay adaptive overcurrent protection scheme for microgrid with distributed generators," *IET G.T.D*, vol. 11, no. 2, pp. 540-549, 2017.
- [6] R. Jain, D. L. Lubkeman, and S. M. Lukic, "Dynamic Adaptive Protection for Distribution Systems in Grid-Connected and Islanded Modes," *IEEE Power Delivery*, vol. 34, no. 1, pp. 281-289, 2019.
- [7] M. G. M. Zanjani, K. Mazlumi, and I. Kamwa, "Application of PMUs for adaptive protection of overcurrent relays in microgrids," *IET G.T.D*, vol. 12, no. 18, pp. 4061-4068, 2018.
- [8] S. Mitra and P. Chattopadhyay, "Design and implementation of flexible Numerical Overcurrent Relay on FPGA," *International Journal of Electrical Power & Energy Systems*, vol. 104, pp. 797-806, 2019.
- [9] H. M. Zeineldin, H. H. Sharaf, and E. El-Saadany, "Protection Coordination for Microgrids with Grid-Connected and Islanded Capabilities using Dual Setting Directional Overcurrent Relays."
- [10] R. Sitharthan, M. Geethanjali, "Adaptive protection scheme for smart microgrid with electronically coupled distributed generations," *Alexandria Engineering Journal*, vol. 55, no. 3, pp. 2539-2550, 2016.
- [11] E. Ebrahimi, M. J. Sanjari, and G. B. Gharehpetian, "Control of three-phase inverter-based DG system during fault condition without changing protection coordination," *International Journal of Electrical Power & Energy Systems*, vol. 63, pp. 814-823, 2014.
- [12] M. A. Zamani, A. Yazdani, and T. S. Sidhu, "A control strategy for enhanced operation of inverter-based microgrids under transient disturbances and network faults," *IEEE Transactions on Power Delivery*, vol. 27, no. 4, pp. 1737-1747, 2012.
- [13] R. R. Ferreira, P. J. Colorado, A. P. Grilo, J. C. Teixeira, and R. C. Santos, "Method for identification of grid operating conditions for adaptive overcurrent protection during intentional islanding operation," *International Journal of Electrical Power & Energy Systems*, vol. 105, pp. 632-641, 2019.
- [14] A. Mehrizi-Sani and R. Iravani, "Potential-function based control of a microgrid in islanded and grid-connected modes," *IEEE Transactions on Power Systems*, vol. 25, no. 4, pp. 1883-1891, 2010.
- [15] L. Che, M. E. Khodayar, and M. Shahidehpour, "Adaptive Protection System for Microgrids: Protection practices of a functional microgrid system," *IEEE Electrification magazine*, vol. 2, no. 1, pp. 66-80, 2014.
- [16] M. Abdel-Salam, A. Abdallah, R. Kamel, and M. Hashem, "Improvement of Protection Coordination for a Distribution System Connected to a Microgrid using Unidirectional Fault Current Limiter," *Ain Shams Engineering Journal*, 2015.
- [17] S. Kar and S. R. Samantaray, "Time-frequency transform-based differential scheme for microgrid protection," *IET Generation, Transmission & Distribution*, vol. 8, no. 2, pp. 310-320, 2014.

Appendix A

In Tables 11-14, the details of micro-grid components including Generators, Transformers, Lines and main grid are shown.

Table 11: Lines Data.

Line Number	Sequences	Nominal Power (MVA)	Rated Voltage (kV)	C (Faraday/km)	L (Henri/km)	R (Ohms/km)	Line Length (km)
DL1, DL2, DL3 DL4, DL5, DL6	positive and negative	20	25	5.01e-9	3.32e-3	0.413	20
	Zero			11.33e-9	1.05e-3	0.1153	

Table 12: Load Data.

Buses Number	1	2	3	4	5
Active Power (MW)	10			6	
Reactive Power (MVAR)	3.5			2.5	

Table 13: Generators Data.

	DG1 , DG3	DG4	DG2	Utility
Type	Synchronous	Inverter Based Wind Farm	DFIG (Doubly Feed Induction Generators)	Main grid
Nominal Power (MVA)	9	4*1.5	6*1.5	1000(SCC)
Power Factor	---	0.9	0.9	
Nominal Voltage (kv)	2.4	0.575	0.575	120
H (s)	1.07	0.62	0.685	
F (pu)	0.1	0.1	0.01	
Rs (pu)	0.0036	0.006	0.023	
X _d (pu)	1.56	1.305	Lls=0.18	
X' _d (pu)	0.296	0.296	Rr'=0.16	
X'' _d (pu)	0.177	0.252	Llr'=0.16	
X _q (pu)	1.06	0.474	Lm=0.16	
X'' _q (pu)	0.177	0.243		
X _l (pu)	0.052	0.18		
T' _d (s)	3.7	4.49		
T'' _d (s)	0.05	0.0681		
T'' _{qo} (s)	0.05	0.513		

